

Syracuse University

**SURFACE**

---

Chemistry - Faculty Scholarship

College of Arts and Sciences

---

4-24-2006

## Dactinomycin Impairs Cellular Respiration and Reduces Accompanying ATP Formation

Zhimin Tao  
*Syracuse University*

Syed S. Ahmad  
*Upstate Medical University*

Harvey S. Penefsky  
*Public Health Research Institute*

Jerry Goodisman  
*Syracuse University*

Abdul Kader Souid  
*Upstate Medical University.*

Follow this and additional works at: <https://surface.syr.edu/che>

 Part of the [Chemistry Commons](#)

---

### Recommended Citation

Tao, Z., Ahmad, S. S., Penefsky, H. S., Goodisman, J., & Souid, A. -. (2006). Dactinomycin impairs cellular respiration and reduces accompanying ATP formation. *Molecular Pharmaceutics*, 3(6), 762-772.

This Article is brought to you for free and open access by the College of Arts and Sciences at SURFACE. It has been accepted for inclusion in Chemistry - Faculty Scholarship by an authorized administrator of SURFACE. For more information, please contact [surface@syr.edu](mailto:surface@syr.edu).

## Dactinomycin Impairs Cellular Respiration and Reduces Accompanying ATP Formation

Zhimin Tao,<sup>†</sup> Syed S. Ahmad,<sup>‡</sup> Harvey S. Penefsky,<sup>§</sup> Jerry Goodisman,<sup>\*,†</sup> and Abdul-Kader Souid<sup>\*,‡</sup>

Department of Chemistry, Syracuse University, 1-014 CST, Syracuse, New York 13244, Department of Pediatrics, State University of New York, Upstate Medical University, Syracuse, New York 13210, and Public Health Research Institute, 225 Warren Street, Newark, New Jersey 07103

Received April 24, 2006

**Abstract:** The effect of dactinomycin on cellular respiration and accompanying ATP formation was investigated in Jurkat and HL-60 cells. Cellular mitochondrial oxygen consumption (measured by a homemade phosphorescence analyzer) and ATP content (measured by the luciferin–luciferase bioluminescence system) were determined as functions of time  $t$  during continuous exposure to the drug. The rate of respiration,  $k$ , was the negative of the slope of  $[O_2]$  versus  $t$ . Oxygen consumption and ATP content were diminished by cyanide, confirming that both processes involved oxidations in the mitochondrial respiratory chain. In the presence of dactinomycin,  $k$  decreased gradually with  $t$ , the decrease being more pronounced at higher drug concentrations. Cellular ATP remained constant for 5 h in untreated cells, but in the presence of 20  $\mu$ M dactinomycin it decreased gradually (to one-tenth the value at 5 h for untreated cells). The drug-induced inhibition of respiration and decrease in ATP were blocked by the pancaspase inhibitor benzyloxycarbonyl-Val-Ala-DL-Asp-fluoromethyl ketone (zVAD-fmk). A rapid but temporary decrease in cellular ATP observed on the addition of zVAD-fmk was shown to be due to DMSO (added with zVAD-fmk). The effect of dactinomycin on respiration differed from that of doxorubicin. Plots of  $[O_2]$  versus  $t$  were curved for dactinomycin so that  $k$  decreased gradually with  $t$ . The corresponding plots for doxorubicin were well fit by two straight lines; so  $k$  was constant for  $\sim 150$  min, at which time  $k$  decreased, remaining constant at a lower level thereafter. The results for cells treated with mixtures of the two drugs indicated that the drugs acted synergistically. These results show the onset and severity of mitochondrial dysfunction in cells undergoing apoptosis induced by dactinomycin.

**Keywords:** Pd phosphor, palladium derivative of *meso*-tetra-(4-sulfonatophenyl)-tetrabenzoporphyrin;  $k$ , zero-order rate constant for cellular oxygen consumption; zVAD-fmk, benzyloxycarbonyl-val-alasp-fluoromethyl ketone

### Introduction

Dactinomycin is an important anticancer chromopeptide.<sup>1</sup> The drug is known to intercalate between DNA base pairs

and inhibit transcription.<sup>2</sup> This toxic effect leads to cell death, primarily by apoptosis. The drug is also commonly used in vitro to execute apoptosis.

Apoptosis is initiated by activating cellular targets (e.g., the pro-apoptotic Bcl-2 family member Bid), which permeabilize the outer mitochondrial membrane, causing release of soluble proteins (e.g., cytochrome *c* and SMAC/Diablo) from the mitochondrial intermembrane space. In the presence of ATP (or dATP), released cytochrome *c* binds to Apaf-1

\* To whom correspondence should be addressed. (J.G.) Tel: 315-443-3035. Fax: 315-443-4070. E-mail: goodisma@mailbox.syr.edu. Address: Department of Chemistry, Syracuse University, 1-014 CST, Syracuse, NY 13244. (A.-K.S.) Tel: 315-464-5294. Fax: 315-464-7238. E-mail: souida@upstate.edu. Address: Department of Pediatrics, State University of New York, Upstate Medical University, Syracuse, NY 13210.

<sup>†</sup> Syracuse University.

<sup>‡</sup> State University of New York, Upstate Medical University.

<sup>§</sup> Public Health Research Institute.

(1) Goldberg, I. H.; Friedman, P. A. Antibiotics and nucleic acids. *Annu. Rev. Biochem.* **1971**, *40*, 775–810.

(2) Muller, W.; Crother, D. M. Studies of the binding of actinomycin and related compounds to DNA. *J. Mol. Biol.* **1968**, *35*, 251–290.

(apoptotic protease-activating factor 1), forming an oligomer (apoptosome) that activates cysteine proteases (caspases).<sup>3</sup> However, cytochrome *c*- and apoptosome-independent pathways for caspase activation are also known.<sup>4</sup>

Apoptosis is executed by caspases, which lead to mitochondrial dysfunction.<sup>5</sup> The mitochondrial perturbation involves opening the permeability transition pores, which are formed at contact sites between the inner and outer mitochondrial membranes. When opened, these pores dissipate the mitochondrial membrane potential ( $\Delta\psi$ ), permit further passage of low-molecular-weight apoptogenic proteins (e.g., cytochrome *c*), and generate reactive oxygen species.<sup>6</sup>

The initial release of cytochrome *c* and dissipation of  $\Delta\psi$  occur in the absence of caspase activities.<sup>7</sup> If caspases are blocked by zVAD-fmk,<sup>8</sup> then the mitochondrial  $\Delta\psi$  can be regenerated despite cytochrome *c* leakage.<sup>9</sup> In the presence of active caspases, mitochondrial dysfunctions remain. The impact of the loss of cytochrome *c* and dissipation of  $\Delta\psi$  on oxidative phosphorylation during apoptosis remains unclear.

We present here the results of measurements of cellular respiration and ATP content during continuous exposure to dactinomycin. The goal of these experiments was to describe the onset and severity of mitochondrial dysfunction in cells undergoing apoptosis in response to dactinomycin. The results show that cyanide-sensitive respiration and accompanying ATP formation are inhibited in cells treated with dactinomycin and that the inhibition is mediated by caspase activity. The effect of dactinomycin on respiration is compared with that of doxorubicin.<sup>10</sup>

- (3) Hengartner, M. O. The biochemistry of apoptosis. *Nature* **2000**, *407*, 770–776.
- (4) Hao, Z.; Duncan, G. S.; Chang, C.-C.; Elia, A.; Fang, M.; Wakeham, A.; Okada, H.; Calzascia, T.; Jang, Y. J.; You-Ten, A.; Yeh, W.-C.; Ohashi, P.; Wang, X.; Mak, T. W. Specific ablation of the apoptotic functions of cytochrome *c* reveals a differential requirement of cytochrome *c* and Apaf-1 in apoptosis. *Cell* **2005**, *121*, 579–591.
- (5) Green, D. R.; Kroemer, G. The pathophysiology of mitochondrial cell death. *Science* **2004**, *305*, 626–629.
- (6) Ricci, J.-E.; Gottlieb, R. A.; Green, D. R. Caspase-mediated loss of mitochondrial function and generation of reactive oxygen species during apoptosis. *J. Cell Biol.* **2003**, *160*, 65–75.
- (7) Goldstein, J. C.; Munoz-Pinedo, J.-E.; Adams, S. R.; Kelekar, A.; Schuler, M.; Tsien, R. Y.; Green, D. R. Cytochrome *c* is released in a single step during apoptosis. *Cell Death Differ.* **2005**, *12*, 453–462.
- (8) Slee, E. A.; Zhu, H.; Chow, S. C.; MacFarlane, M.; Nicholson, D. W.; Cohen, G. M. Benzylloxycarbonyl-Val-Ala-Asp (Ome) fluoromethyl ketone (Z-VAD-FMK) inhibits apoptosis by blocking the processing of CPP32. *Biochem. J.* **1996**, *315*, 21–4.
- (9) Waterhouse, N. J.; Sedelies, K. A.; Sutton, V. R.; Pinkoski, M. J.; Thia, K. Y.; Johnstone, R.; Bird, P. I.; Green, D. R.; Trapani, J. A. Functional dissociation of  $\Delta\psi$  and cytochrome *c* release defines the contribution of mitochondria upstream of caspase activation during granzyme B-induced apoptosis. *Cell Death Differ.* **2006**, *13*, 607–618.
- (10) Tao, Z.; Withers, H. G.; Penefsky, H. S.; Ahmad, S. S.; Goodisman, J.; Souid, A.-K. Inhibition of cellular respiration by doxorubicin. *Chem. Res. Toxicol.* **2006**, *19*, 1051–1058.

## Materials and Experimental Procedures

**Chemicals.** Dactinomycin (actinomycin D,  $M_w$  1255.43) was purchased from Merck (Whitehouse Station, NJ). The Pd(II) complex of *meso*-tetra-(4-sulfonatophenyl)-tetrabenzoporphyrin (Pd phosphor sodium salt) was purchased from Porphyrin Products (Logan, UT). Fetal bovine serum and RPMI-1640 medium<sup>10–040</sup> with L-glutamine (pH 7.15  $\pm$  0.1) were purchased from Mediatech (Herndon, VA). Jurkat clone E6-1 human acute T-cell leukemia (TIB-152) and human leukemia-60 (HL-60) were purchased from American Tissue Culture Collection (Manassas, VA). The luciferin–luciferase mixture (0.2 mg luciferin and 22 000 units luciferase per vial, stored at  $-20^\circ\text{C}$ ) and ATP (2 micromol per vial, stored at  $-20^\circ\text{C}$ ) were purchased from Chrono-Log (Havertown, PA). Caspase inhibitor I (zVAD-fmk,  $M_w$  467.5) was purchased from Calbiochem (San Diego, CA). The remaining reagents were purchased from Sigma-Aldrich (St. Louis, MO).

**Solutions.** Dactinomycin solution was made fresh in  $\text{dH}_2\text{O}$ ; its final concentration was determined by absorbance at 440 nm using an extinction coefficient of 24 450  $\text{M}^{-1}\text{cm}^{-1}$ . Aqueous solution of ATP (0.4 mM) was made fresh in 10 mM Tris-HEPES (pH 7.5); its final concentration was determined by absorbance at 259 nm using an extinction coefficient of 15 400  $\text{M}^{-1}\text{cm}^{-1}$ .<sup>11–12</sup> A working solution of ATP (4  $\mu\text{M}$ ) was prepared immediately prior to use in 0.1 M Tris-HEPES (pH 7.5), 5 mM  $\text{MgCl}_2$ , and 0.1% fat-free bovine serum albumin. A lyophilized powder containing luciferin (0.2 mg,  $M_w$  280) and luciferase (22 000 units) was freshly dissolved in 1.25 mL PBS, protected from light, and placed on ice. The final concentration of luciferin (570  $\mu\text{M}$ ) was determined by absorbance at 327 nm using an extinction coefficient of 18 000  $\text{M}^{-1}\text{cm}^{-1}$ .<sup>12</sup> NaCN solution was freshly prepared at 1.0 M and brought to pH 7.5 with 6N HCl. The zVAD-fmk solution was made by dissolving 1.0 mg in 1.0 mL DMSO (final concentration, 2.14 mM) and stored at  $-20^\circ\text{C}$ .

**Cells.** The measurements were made on Jurkat and HL-60 cells. The cells were maintained in suspension cultures as described.<sup>10</sup> The cell count and viability were determined by light microscopy using a hemocytometer under standard trypan blue staining conditions.

**Incubation with Drugs.** A fresh solution of RPMI-1640 medium (containing 6 mM  $\text{Na}_2\text{HPO}_4$  and 10 mM glucose), 10% fetal bovine serum, 2  $\mu\text{M}$  Pd phosphor and 1% fat-free bovine serum albumin was stirred vigorously at  $37^\circ\text{C}$  for 30 min. Cells (usually  $0.5 \times 10^6$  cells/mL) were suspended in this solution and incubated at  $37^\circ\text{C}$  with gentle stirring. The drugs (dactinomycin, doxorubicin, zVAD-fmk, and/or NaCN) were then added. For each condition, 1 mL of the cell suspension was placed in a 1 mL glass vial (8 mm clear

- (11) Karamohamed, S.; Guidotti, G. Bioluminometric method for real-time detection of ATPase activity. *BioTechniques* **2001**, *31*, 420–425.
- (12) Lemasters, J. J.; Hackenbrock, C. R. Continuous measurements of adenosine triphosphate with firefly luciferase luminescence. *Method Enzymol.* **1979**, *56*, 530–544.

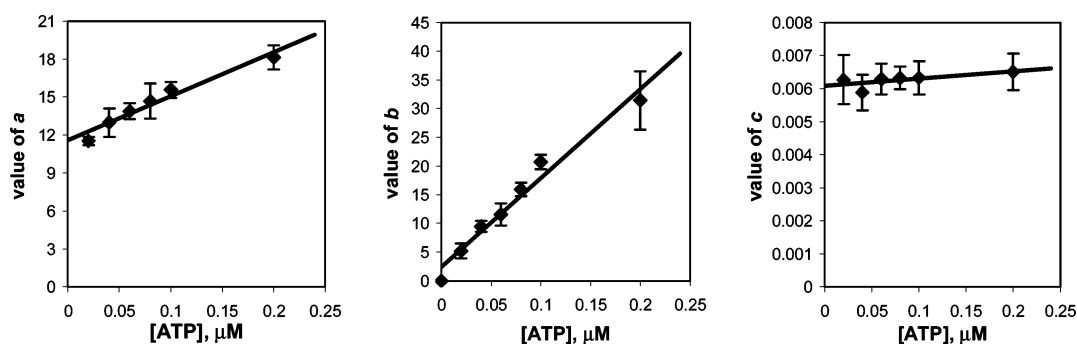


**Figure 1.** Calibration of the luminometer. The luminescence intensities of solutions of known ATP concentrations were determined as a function of  $t$  and fitted to the expression:  $a + be^{-ct}$ . Shown are values of  $a$ ,  $b$ , and  $c$  (mean  $\pm$  SD) for various  $[ATP]$ , with linear fits. The fit to a plot of  $b$  vs  $[ATP]$ , with the point for  $[ATP] = 0.20 \mu\text{M}$  removed, was used to convert measured  $b$  to  $[ATP]$  for unknowns.

vials, Krackler Scientific, Albany, NY). The vials were sealed with a crimp-top aluminum seal and placed in the instrument for  $\text{O}_2$  measurements at  $37^\circ\text{C}$ . Mixing was done with the aid of parylene-coated stir bars (V&P Scientific, Inc., San Diego, CA).

**Cellular Respiration.**  $[\text{O}_2]$  in the suspension was determined as a function of  $t$  using the phosphorescence of Pd (II) meso-tetra-(4-sulfonatophenyl)-tetrabenzoporphyrin.<sup>13</sup> The decay of Pd phosphor phosphorescence intensity,  $I$ , with  $t$  was exponential,  $I = Ae^{-t/\tau}$ . The reciprocal of the phosphorescence decay time ( $\tau$ ) was linear in  $[\text{O}_2]$ ,  $1/\tau = 1/\tau^\circ + k_q[\text{O}_2]$ . Here,  $\tau$  is the lifetime in the presence of  $\text{O}_2$ ,  $\tau^\circ$  is the lifetime in the absence of  $\text{O}_2$ , and  $k_q$  is the second-order  $\text{O}_2$  quenching rate constant. The instrument was calibrated with ascorbate and ascorbate oxidase as described earlier.<sup>10,13–14</sup> The value of  $k_q$  ( $96.1 \pm 1.2 \mu\text{M}^{-1} \text{s}^{-1}$ ) was determined from the slope of the plot of  $1/\tau$  versus  $[\text{O}_2]$ ; the value of  $1/\tau^\circ$  ( $10\,087 \pm 156 \text{s}^{-1}$ ) was the plot intercept. The equation  $1/\tau = 1/\tau^\circ + k_q[\text{O}_2]$  was then used to calculate  $[\text{O}_2]$  from measured  $\tau$ .<sup>10</sup> The rate of respiration  $k$ , in  $\mu\text{M} \text{O}_2 \text{min}^{-1}$ , was determined as the negative slope of the curve of  $[\text{O}_2]$  versus  $t$ .

The measurements of  $[\text{O}_2]$  began  $\sim 20$ – $30$  min after the addition of dactinomycin; this time was required for simultaneous processing of the samples, placing the mixtures in glass vials, eliminating air bubbles, sealing the vials, cleaning them, warming them up to  $37^\circ\text{C}$ , placing them in the instrument, and starting the program. Variations in  $k$  between different cell batches were sometimes noted. Thus, it was important to use cells from the same batch when the  $k$  values for different conditions were to be compared.

Addition of  $10 \text{ mM NaCN}$  during measurements of cellular respiration resulted in  $\sim 90\%$  inhibition of  $\text{O}_2$  uptake. The

apparent value of  $k$  after the addition of cyanide was close to the value found for cyanide in media without cells, indicating that the decline in  $[\text{O}_2]$  following the addition of cyanide was artifactual, possibly a drift in the instrument or direct reaction of cyanide with  $\text{O}_2$ . Thus, the decline in  $[\text{O}_2]$  with time in the presence of cells reflected mainly cellular mitochondrial  $\text{O}_2$  consumption.

**Cellular ATP Content.** Cellular ATP content was measured using the luciferin–luciferase bioluminescence system.<sup>11–12</sup> Cellular acid extracts were prepared by adding  $200 \mu\text{L}$  of  $10\%$  perchloric acid to each pellet of  $0.5 \times 10^6$  cells. After sonication of the mixture on ice for  $30 \text{ s}$ , we collected the supernatant by centrifugation and neutralized it by adding  $200 \mu\text{L}$  of  $2 \text{ M KOH}$ . The sample was incubated on ice for  $15 \text{ min}$ , and the precipitated  $\text{KClO}_4$  was removed by centrifugation. The ATP content of the resulting supernatant was determined from the decay of luciferin bioluminescence.

Luminescence was measured at  $37^\circ\text{C}$  using a luminometer (Chrono-Log Corporation, Havertown, PA) connected to the Chrono-log AGGRO/LINK interface. The data were exported into Microsoft Excel and analyzed as described below. The reaction mixture contained, in a final volume of  $0.4 \text{ mL}$ ,  $0.1 \text{ M Tris-HEPES}$  ( $\text{pH } 7.6$ ),  $5 \text{ mM MgCl}_2$ ,  $0.1\%$  fat-free bovine serum albumin, and ATP ( $40$ – $120 \text{ pmol}$ ) or cell acid extract ( $10 \mu\text{L}$ ). The reaction was started by rapidly injecting  $10 \mu\text{L}$  of luciferin/luciferase mixture ( $5 \text{ nmol}$  luciferin and  $176$  units luciferase) from a  $50 \mu\text{L}$  Hamilton syringe into  $0.4 \text{ mL}$  of rapidly stirred assay mixture.

The luminometer was calibrated as follows: For known concentrations of ATP between  $0$  and  $0.2 \mu\text{M}$ , plots of luminescence intensity  $I$  versus  $t$  were obtained, intensity being measured every  $0.5 \text{ s}$  out to  $300$ – $600 \text{ s}$ . The plots were well fit to the three-parameter function,  $I = a + be^{-ct}$ . Figure 1 shows the resulting values of  $a$ ,  $b$ , and  $c$  (each value is the average of  $3$ – $4$  experiments, with the standard deviation shown by the error bars) plotted versus  $[ATP]$ , with best-fit straight lines. It is clear that the decay constant,  $c$ , is independent of  $[ATP]$ , being a property of the luciferin/luciferase system, whereas the other two parameters increase linearly with  $[ATP]$ . Because  $b$  but not  $c$  is close to zero for

(13) Lo, L.-W.; Koch, C. J.; Wilson, D. F. Calibration of oxygen-dependent quenching of the phosphorescence of Pd-meso-tetra-(4-carboxyphenyl) porphine: A phosphor with general application for measuring oxygen concentration in biological systems. *Anal. Biochem.* **1996**, *236*, 153–160.

(14) Souid, A.-K.; Tacka, K. A.; Galvan, K. A.; Penefsky, H. S. Immediate effects of anticancer drugs on mitochondrial oxygen consumption. *Biochem. Pharmacol.* **2003**, *66*, 977–987.



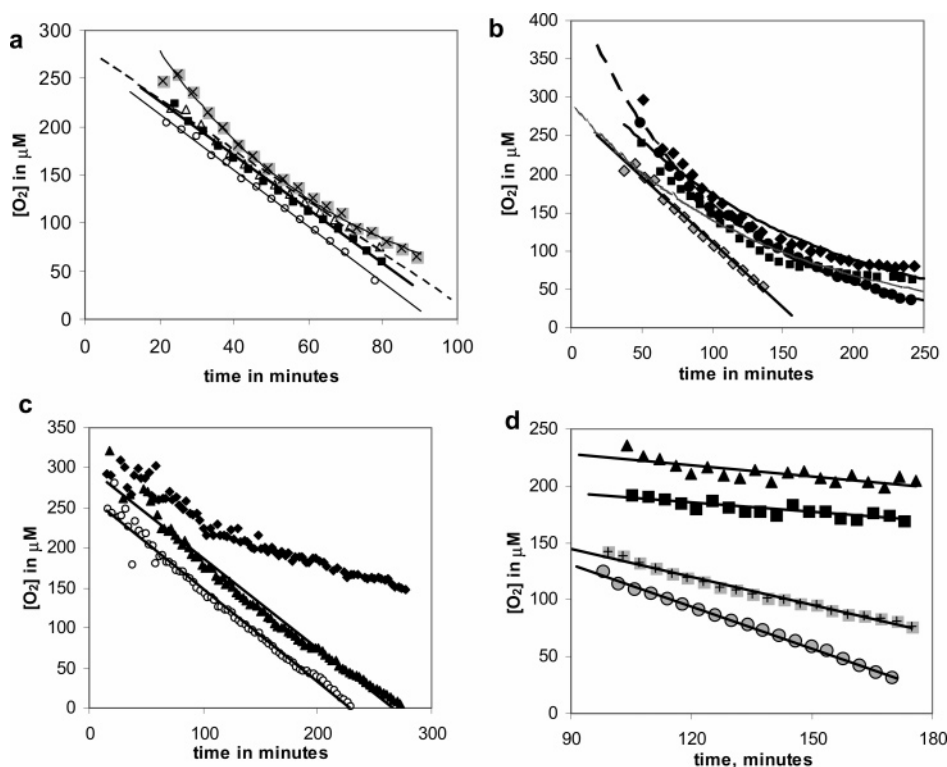


**Figure 2.** Dactinomycin inhibits Jurkat cell respiration. (a) Cells were suspended at  $10^6$  cells/mL of media, 10% fetal bovine serum,  $2 \mu\text{M}$  Pd phosphor, and 1% albumin with and without dactinomycin. One milliliter of each suspension was placed in a 1.0 mL glass vial, which was then sealed and placed in the instrument for  $[\text{O}_2]$  measurements. Best-fit lines are shown. Circles, cells alone; triangles and dashed line, cells plus  $3 \mu\text{M}$  dactinomycin; squares and heavy line, cells plus  $5 \mu\text{M}$  dactinomycin; X's with exponential fit, cells plus  $10 \mu\text{M}$  dactinomycin. (b) Cells were suspended at  $0.5 \times 10^6$  cells/mL with and without dactinomycin and processed as in part a. Grey diamonds and heavy line (linear fit), cells alone; circles and dashed curve, cells plus  $10 \mu\text{M}$  dactinomycin; dark squares and curve, cells plus  $20 \mu\text{M}$  dactinomycin; diamonds and light curve, cells plus  $40 \mu\text{M}$  dactinomycin. All curves are exponential fits. (c) Effect of zVAD-fmk ( $0.5 \times 10^6$  cells/mL). Circles, cells alone (with linear fit); diamonds, cells plus  $20 \mu\text{M}$  dactinomycin; triangles, cells plus  $20 \mu\text{M}$  dactinomycin plus  $20 \mu\text{M}$  zVAD (with linear fit). (d) Effect of NaCN after 90 min ( $0.5 \times 10^6$  cells/mL). Circles, untreated cells (with linear fit); gray squares with +, cells plus  $10 \mu\text{M}$  dactinomycin (with linear fit); triangles, cells plus  $10 \text{ mM}$  NaCN (with linear fit); squares, cells plus  $10 \mu\text{M}$  dactinomycin plus  $10 \text{ mM}$  NaCN (with linear fit). In all experiments, minute zero corresponded to the addition of drug.

$[\text{ATP}] = 0$  (the line is  $b = 2.40 + 155[\text{ATP}]$ ,  $r^2 = 0.970$ ),  $b$  is an appropriate measure of  $[\text{ATP}]$ . For increased accuracy, we use only results for  $[\text{ATP}] \leq 0.1 \mu\text{M}$ , which yield the line  $b = 0.62 + 197[\text{ATP}]$ ,  $r^2 = 0.990$ . When applying this calibration to the measurement of unknowns, it was sometimes necessary to dilute cell acid extracts to obtain  $b < 25$ , or  $[\text{ATP}] < 0.12 \mu\text{M}$ .

## Results

**Dactinomycin Decreases Cellular Respiration.** Figure 2 shows the effect of dactinomycin on Jurkat cell respiration. Results for Jurkat cells ( $10^6$  cells/mL) in the presence of 0, 3, 5, and  $10 \mu\text{M}$  dactinomycin are shown in Figure 2a. For untreated cells (circles),  $[\text{O}_2]$  was a linear function of  $t$  (slope =  $-3.12 \mu\text{M O}_2 \text{ min}^{-1}$ ,  $r^2 = 0.994$ ). The rate of respiration,  $k$ , the negative of the slope, was thus constant. For cells treated with 3 and  $5 \mu\text{M}$  of drug (triangles and squares, respectively), the slopes (dashed and heavy lines, respectively) were  $-2.68 \mu\text{M O}_2 \text{ min}^{-1}$  ( $r^2 = 0.988$ ) and  $-2.83 \mu\text{M O}_2 \text{ min}^{-1}$  ( $r^2 = 0.996$ ), respectively. With  $10 \mu\text{M}$  drug (X's in gray squares), the slope gradually became less

negative with time; the best exponential fit is shown in Figure 2a. We also found the best linear fits to the first 13 data points ( $t < 70$  min) and the last 17 data points ( $t > 70$  min). The slope of the first was  $-3.18 \mu\text{M O}_2 \text{ min}^{-1}$  ( $r^2 = 0.978$ ), the same as that for untreated cells, and the slope of the second was  $-2.10 \mu\text{M O}_2 \text{ min}^{-1}$  ( $r^2 = 0.997$ ),  $\sim 1/3$  lower.

$[\text{O}_2]$  as a function of  $t$  for Jurkat cell respiration in the presence of higher  $[\text{dactinomycin}]$  is shown in Figure 2b. For these experiments,  $0.5 \times 10^6$  cells/mL were used. For untreated cells (grey diamonds), the linear fit ( $r^2 = 0.991$ , shown as a dark line) had a slope of  $-1.70 \mu\text{M O}_2 \text{ min}^{-1}$ , somewhat more than half the slope of Figure 2a (circles), since only half the number of cells were used here as in Figure 2a. The circles, squares, and diamonds are results for cells treated with 10, 20, and  $40 \mu\text{M}$  dactinomycin, respectively. It is clear here that the plots of  $[\text{O}_2]$  as functions of  $t$  are not linear. The value of  $k$  decreased gradually with  $t$  (best-fit exponentials are shown). Using the last five points for each concentration, we could obtain slopes for large values of  $t$ . For  $10 \mu\text{M}$  dactinomycin, the slope was  $-0.58$

$\mu\text{M O}_2 \text{ min}^{-1}$ , about  $1/3$  of that for untreated cells. For both 20 and 40  $\mu\text{M}$  dactinomycin, the slopes were  $-0.11 \mu\text{M O}_2 \text{ min}^{-1}$ , a 94% decrease from the value for untreated cells. The fact that the slopes were the same for 20 and 40  $\mu\text{M}$  suggested that a limiting value had been reached.

The inhibition of cellular respiration by dactinomycin is not a direct effect on the mitochondria but is mediated by caspase activation. This is shown by the fact that it was completely blocked when 20  $\mu\text{M}$  zVAD-fmk was present in the incubation mixture (Figure 2c). In these experiments,  $0.5 \times 10^6$  Jurkat cells/mL were used. For untreated cells (circles), the best-fit line ( $r^2 = 0.985$ ) had a slope of  $-1.157 \mu\text{M O}_2 \text{ min}^{-1}$ . For cells treated with 20  $\mu\text{M}$  dactinomycin (diamonds),  $[\text{O}_2]$  versus  $t$  showed the curved shape characteristic of the inhibition of respiration by dactinomycin, the slope becoming gradually less negative with  $t$ . When 20  $\mu\text{M}$  zVAD-fmk was included in the incubation mixture with 20  $\mu\text{M}$  dactinomycin (triangles), the plot of  $[\text{O}_2]$  versus  $t$  became linear again, with the best-fit line ( $r^2 = 0.983$ ) having a slope of  $-1.127 \mu\text{M O}_2 \text{ min}^{-1}$ , essentially the same as that for untreated cells. Thus, because addition of the caspase inhibitor blocked the effect, it is clear that caspase activities were responsible for the inhibition of respiration.

The inhibitory effect of NaCN is shown in Figure 2d. In these experiments,  $0.5 \times 10^6$  Jurkat cells/mL were used. The  $[\text{O}_2]$  for untreated cells for  $t > 90$  min are shown by the circles, with a linear fit. The slope ( $r^2 = 0.9968$ ) was  $-1.222 \mu\text{M O}_2/\text{min}$ ; the same value was obtained if points for  $t < 90$  min were included. For cells treated with 10  $\mu\text{M}$  dactinomycin (+ in light squares), the slope ( $r^2 = 0.9869$ ) was  $-0.828 \mu\text{M O}_2 \text{ min}^{-1}$ , a 32% decrease from the value for untreated cells. The slope of the oxygen curve for cells treated with 10 mM NaCN was  $-0.32 \mu\text{M O}_2 \text{ min}^{-1}$ , and the slope of the oxygen curve for cells treated with both NaCN and dactinomycin was  $-0.29 \mu\text{M O}_2 \text{ min}^{-1}$ , the same within experimental error. Thus, NaCN reduced respiration to the same level for dactinomycin-treated and untreated cells. The rate of decrease of  $[\text{O}_2]$  observed in the control Pd phosphor solution (without cells) containing 10 mM NaCN alone was about  $0.10 \mu\text{M O}_2 \text{ min}^{-1}$ . Thus, NaCN almost fully impaired cellular respiration in these experiments.

We next compared the respiration of Jurkat and HL-60 cells in the presence of dactinomycin. The results are shown in Figure 3. The incubation mixture contained  $10^6$  cells/mL. For comparison, Figure 3a shows measured  $[\text{O}_2]$  as a function of  $t$  for Jurkat cells exposed to 0, 3, 5, and 10  $\mu\text{M}$  dactinomycin (circles, squares, triangles, and X's, respectively). For 0, 3, and 5  $\mu\text{M}$  dactinomycin, the oxygen consumption curves were fit by straight lines ( $r^2 = 0.997$ , 0.991, and 0.995, respectively) with slopes of  $-2.92 \mu\text{M O}_2 \text{ min}^{-1}$ ,  $-2.66 \mu\text{M O}_2 \text{ min}^{-1}$ , and  $-2.82 \mu\text{M O}_2 \text{ min}^{-1}$ , respectively. For 10  $\mu\text{M}$  dactinomycin, the curve was no longer linear (the best-fit exponential is shown). Figure 3b shows  $[\text{O}_2]$  as a function of  $t$  for HL-60 cells, either untreated (circles) or treated with 3  $\mu\text{M}$  dactinomycin (squares). For the untreated cells,  $[\text{O}_2]$  decreased linearly with  $t$  ( $r^2 = 0.993$ ); the slope of the best-fit line as shown was  $-0.55$

$\mu\text{M O}_2 \text{ min}^{-1}$  (significantly lower than that for untreated Jurkat cells). For the cells treated with 3  $\mu\text{M}$  dactinomycin, the positive curvature in the  $[\text{O}_2]$  versus  $t$  curve showed that the respiration rate decreased with  $t$  for HL-60, as for Jurkat cells. However, the effect was evident at a much lower concentration (3 vs 10  $\mu\text{M}$ ), indicating a greater sensitivity to dactinomycin for the HL-60 cells.

HL-60 cells were suspended in media with 10% fetal bovine serum, 2  $\mu\text{M}$  Pd phosphor, and 1% albumin and incubated in open containers at 37 °C with or without 3  $\mu\text{M}$  dactinomycin. Aliquots of untreated and treated cells were taken periodically for respiration measurement. Because the duration of each measurement was short,  $[\text{O}_2]$  decreased linearly with  $t$  for treated or untreated cells. The results are in Figure 3c. For untreated cells (circles), the values of  $d[\text{O}_2]/dt$  from the linear fits were (from left to right)  $-0.49 \pm 0.02$ ,  $-0.65 \pm 0.06$ , and  $-0.79 \pm 0.06 \mu\text{M O}_2 \text{ min}^{-1}$  (statistical errors from linear fits); the increase in  $k$  may reflect cell growth. For treated cells (squares), the values of  $d[\text{O}_2]/dt$  from the linear fits were (from left to right)  $-0.26 \pm 0.01$ ,  $-0.27 \pm 0.02$ , and  $-0.29 \pm 0.01 \mu\text{M O}_2 \text{ min}^{-1}$  (statistical errors from linear fits). Thus,  $k$  is reduced by 47%, 58%, and 73% after 50, 150, and 270 min of incubation (times at which samples were taken for  $\text{O}_2$  measurement).

Figure 3d shows the results of respiration measurements on HL-60 cells either untreated or treated with 2.0  $\mu\text{M}$  or 3.7  $\mu\text{M}$  dactinomycin. Starting at different times after addition of drug,  $[\text{O}_2]$  was measured for small time intervals as in Figure 3c. During each interval,  $[\text{O}_2]$  decreased linearly with  $t$ , allowing determination of  $k = -d[\text{O}_2]/dt$ . The curves of Figure 3d were generated by fitting measured  $k$  as a function of incubation time to an exponential (circles and dotted line, untreated cells; squares and dashed line, cells treated with 2.0  $\mu\text{M}$  dactinomycin; triangles and curved line, cells treated with 3.7  $\mu\text{M}$  dactinomycin). Clearly, the positive curvature increases with increased [dactinomycin].

**Dactinomycin Lowers Cellular ATP.** The results of cellular ATP measurements are shown in Figure 4. Jurkat cells were suspended at  $0.5 \times 10^6$  cells/mL media with 10% fetal bovine serum and 1% albumin and incubated at 37 °C for up to 5 h, open to air. Three conditions were used: no additions, with 20  $\mu\text{M}$  dactinomycin (which strongly inhibited respiration), and with 20  $\mu\text{M}$  dactinomycin plus 50  $\mu\text{M}$  zVAD-fmk (a combination that was without effect on respiration). At 1 h intervals after addition of dactinomycin, 1.0 mL samples of each cell suspension were taken for ATP analysis. As shown in Figure 4a, for untreated cells (diamonds), the cellular ATP level remained constant with  $t$ , consistent with the constant rate of respiration discussed above. The linear fit to the ATP levels exhibited a slope of zero within statistical error ( $-0.15 \pm 0.22 \text{ nmol ATP min}^{-1}$  for  $0.5 \times 10^6$  cells). The average ATP level with standard deviation was  $7.25 \pm 0.85 \text{ nmol}$ . The presence of 20  $\mu\text{M}$  dactinomycin (black squares) led to a gradual decrease in cellular ATP, consistent with the gradual decrease in respiration observed with this drug (Figures 2 and 3). The presence of 20  $\mu\text{M}$  dactinomycin and 50  $\mu\text{M}$  zVAD-fmk

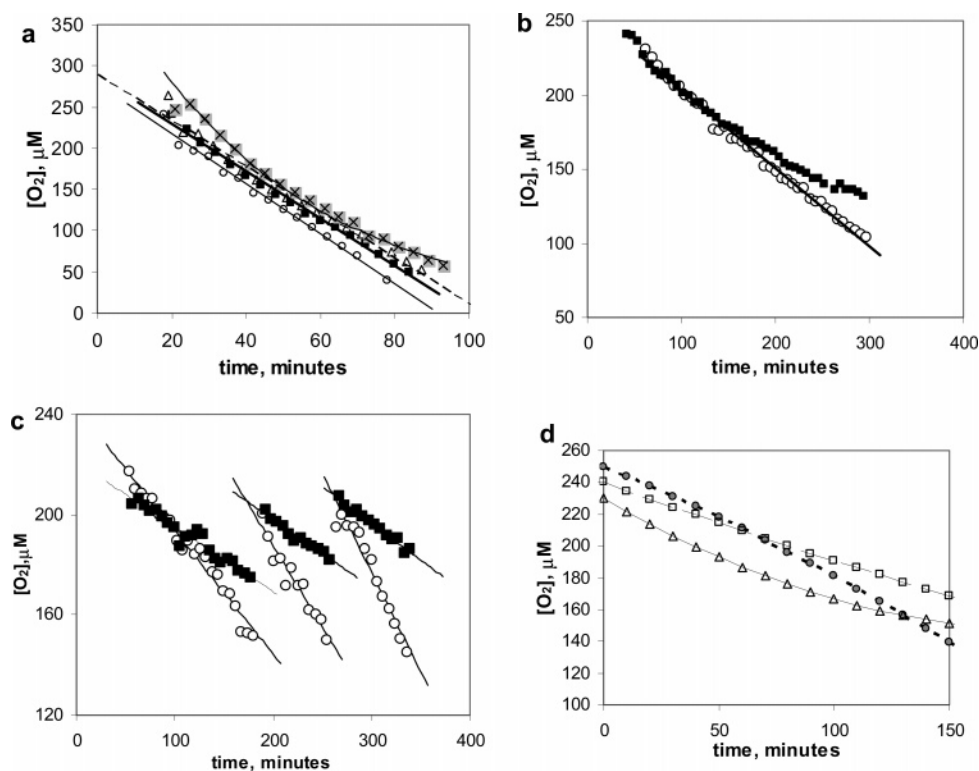


**Figure 3.** Comparing dactinomycin-induced inhibition of Jurkat cell respiration to that of HL-60 cells. Cells were suspended at  $10^6$  cells/mL with and without dactinomycin and processed as in Figure 2a. (a)  $[O_2]$  as a function of  $t$  for Jurkat cells. Circles and best-fit straight line, cells alone; squares and heavy line, cells plus  $3 \mu\text{M}$  dactinomycin; triangles and dashed line, cells plus  $5 \mu\text{M}$  dactinomycin; X's and curved line (best-fit exponential), cells plus  $10 \mu\text{M}$  dactinomycin. (b)  $[O_2]$  as a function of  $t$  for HL-60 cells. Circles, cells alone (with best-fit straight line); squares, cells plus  $3 \mu\text{M}$  dactinomycin. The curvature, showing gradually decreasing respiration, is evident even at this low concentration. (c) Cells were incubated with and without  $3 \mu\text{M}$  dactinomycin in the presence of air. Periodically, 1.0 mL of the cell suspension ( $10^6$  HL-60 cells/mL) was transferred to a 1 mL glass vial and processed for  $[O_2]$  measurements. Circles, no dactinomycin (with best-fit straight lines); squares, cells plus  $3 \mu\text{M}$  dactinomycin (with best-fit straight lines). Minute zero corresponded to the addition of dactinomycin. (d) Results of respiration measurements on HL-60 cells ( $10^6$  cells/mL) either untreated (circles + dotted line), treated with  $2 \mu\text{M}$  dactinomycin (squares + dashed line), or treated with  $3.7 \mu\text{M}$  dactinomycin (triangles + curved line). Curves created by fitting  $k$  values obtained at different  $t$ .

(grey squares) produced a rapid decrease in ATP level (by 46% after 1 h), which was followed by recovery to a level slightly below that for untreated cells by 4 h.

The rapid decrease in ATP level for cells treated with dactinomycin + zVAD-fmk could not be due to a decrease in respiration rate because (i) the ATP level subsequently recovered almost to the level for untreated cells, (ii) no decrease in respiration was observed for cells incubated with dactinomycin + zVAD-fmk, and (iii) ATP levels did not decrease after 1 h when cells were treated with dactinomycin alone. The results of Figure 4b show that the decline in ATP level was associated with DMSO, which was introduced with the zVAD-fmk. We measured ATP content in  $0.5 \times 10^6$  Jurkat cells under the following three conditions: addition of DMSO ( $23 \mu\text{L}$ ) only (squares), addition of DMSO ( $23 \mu\text{L}$ ) plus  $10 \mu\text{M}$  dactinomycin (circles), and addition of zVAD-fmk (in  $23 \mu\text{L}$  DMSO) plus  $10 \mu\text{M}$  dactinomycin (triangles). A marked decrease in ATP level is shown during the first hour after addition for all three conditions. All three conditions showed a subsequent recovery of ATP, which was

more noticeable in the absence of dactinomycin. Thus, it is likely that DMSO produced a transient cellular ATP leakage.

Addition of 10 mM NaCN to the cell suspension resulted in a greater than 90% decrease in cellular ATP level at 1 h. The level of ATP remained unmeasurable out to 5 h, thus establishing that the process of ATP synthesis occurred primarily in the respiratory chain.

**Combination of Dactinomycin and Doxorubicin.** When cells were treated with dactinomycin, the rate of respiration decreased gradually, starting at the time of drug addition (Figures 2-3). In contrast, respiration in the presence of doxorubicin remained unchanged until about 150 min; it then decreased to a lower constant value.<sup>10</sup> In Figure 5, we present the results for cells treated with mixtures of the two drugs.  $[O_2]$  was measured for  $0.5 \times 10^6$  Jurkat cells/mL under six conditions: (1) cells alone, (2) cells plus  $10 \mu\text{M}$  doxorubicin, (3) cells plus  $20 \mu\text{M}$  doxorubicin, (4) cells plus  $10 \mu\text{M}$  dactinomycin, (5) cells plus  $20 \mu\text{M}$  dactinomycin, and (6) cells plus  $10 \mu\text{M}$  doxorubicin plus  $10 \mu\text{M}$  dactinomycin. For clarity, the results are divided between Figure 5a and b.

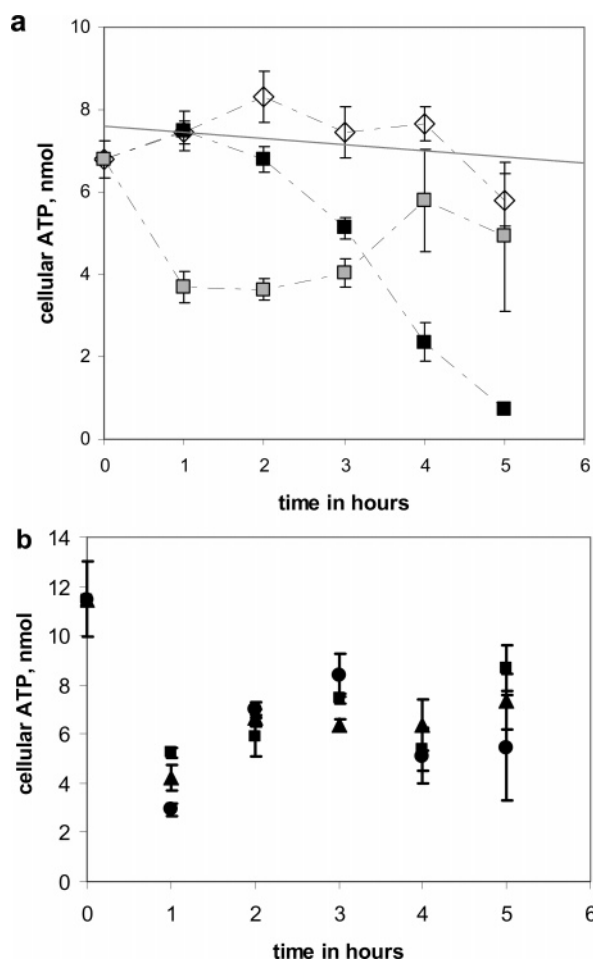


**Figure 4.** Measured cellular ATP levels, in nmol ATP for  $0.5 \times 10^6$  Jurkat cells, as a function of incubation time  $t$ . Minute zero corresponded to the addition of dactinomycin. (a) Diamonds for untreated cells, with best-fit line having zero slope; black squares for cells treated with  $20 \mu\text{M}$  dactinomycin, which produces a gradual decrease in respiration with  $t$ ; gray squares for cells treated with  $20 \mu\text{M}$  dactinomycin +  $50 \mu\text{M}$  zVAD-fmk. The early decrease in ATP level in the presence of zVAD-fmk is due to the DMSO, which is introduced with the zVAD-fmk. (b) ATP levels for cells treated with DMSO (filled squares), DMSO + dactinomycin (filled circles), and zVAD-fmk + dactinomycin (filled triangles). Introduction of zVAD-fmk also introduces DMSO. These results show that the early decrease in ATP when zVAD-fmk is added is due to the DMSO associated with zVAD-fmk.

In Figure 5a,  $[\text{O}_2]$  for untreated cells is shown as circles, with the best-fit line having a slope of  $-0.9731 \mu\text{M O}_2 \text{ min}^{-1}$  ( $r^2 = 0.990$ ). Addition of  $10 \mu\text{M}$  doxorubicin (Figure 5a, open squares) produced no noticeable effect; the best-fit line had a slope of  $-0.9778 \mu\text{M O}_2 \text{ min}^{-1}$  ( $r^2 = 0.997$ ). With  $20 \mu\text{M}$  doxorubicin (triangles), the effect was noticeable; the best-fit line (not shown) using all data points had a slope of  $-0.8575 \mu\text{M O}_2 \text{ min}^{-1}$  ( $r^2 = 0.982$ ). As noted above, oxygen consumption curves in the presence of doxorubicin characteristically consisted of two lines with a change in slope, corresponding to a lower rate of respiration, at  $\sim 150$  min. The dashed lines in Figure 5a are linear fits to the  $[\text{O}_2]$  for

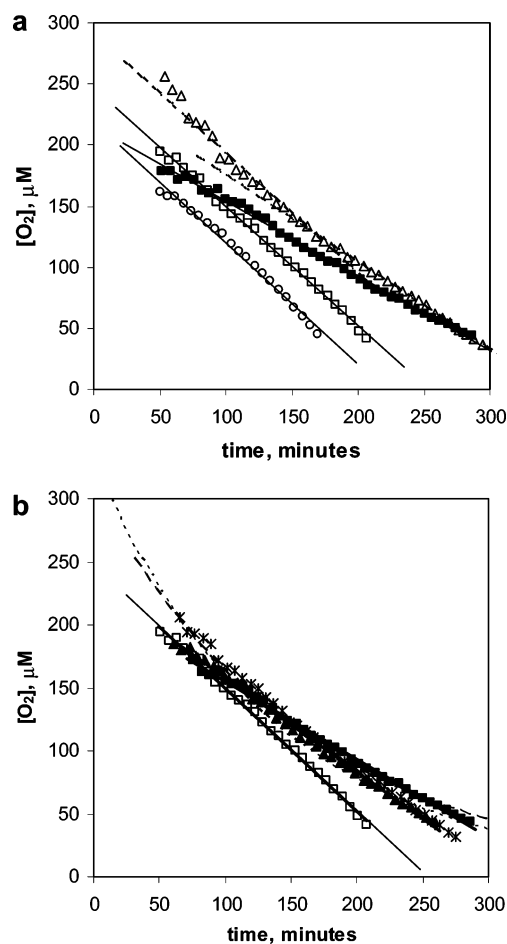


**Figure 5.**  $[\text{O}_2]$  as a function of  $t$  for  $0.5 \times 10^6$  Jurkat cells in the presence of dactinomycin and/or doxorubicin. (a) Circles, cells alone (with best-fit straight line); open squares, cells plus  $10 \mu\text{M}$  doxorubicin (with best-fit straight line); triangles and broken lines, cells plus  $20 \mu\text{M}$  doxorubicin (with linear fits to the data up to 162 min and to the data after 162 min); filled squares, cells plus  $10 \mu\text{M}$  dactinomycin (with best-fit straight line). (b) Open squares, cells plus  $10 \mu\text{M}$  doxorubicin (with best-fit straight line); filled squares and long-dashed curve, cells plus  $10 \mu\text{M}$  dactinomycin (with best-fit exponential); triangles and short-dashed curve, cells plus  $20 \mu\text{M}$  dactinomycin (with best-fit exponential); stars, cells plus  $10 \mu\text{M}$  doxorubicin plus  $10 \mu\text{M}$  dactinomycin.

$t < 163$  min (slope =  $-0.983 \mu\text{M O}_2 \text{ min}^{-1}$ ,  $r^2 = 0.956$ , the same as that of untreated cells) and to the  $[\text{O}_2]$  for  $t > 163$  min (slope =  $-0.712 \mu\text{M O}_2 \text{ min}^{-1}$ ,  $r^2 = 0.998$ , a 28% decrease). The filled squares in Figure 5a are for condition 4, exposure to  $10 \mu\text{M}$  dactinomycin. The plot curvature was slight due to the lack of measurements at  $t < 50$  min; the linear fit had a slope of  $-0.610 \mu\text{M O}_2 \text{ min}^{-1}$  ( $r^2 = 0.996$ ). The lowering of  $k$  by  $10 \mu\text{M}$  dactinomycin was 37%, larger than the lowering by  $10 \mu\text{M}$  doxorubicin, showing that dactinomycin was more potent at reducing respiration.

Figure 5b shows the oxygen consumption curves for conditions 2, 4, 5, and 6, listed above. The  $10 \mu\text{M}$  doxorubicin condition (open squares) was discussed above. The 10 and  $20 \mu\text{M}$  dactinomycin results (filled squares and



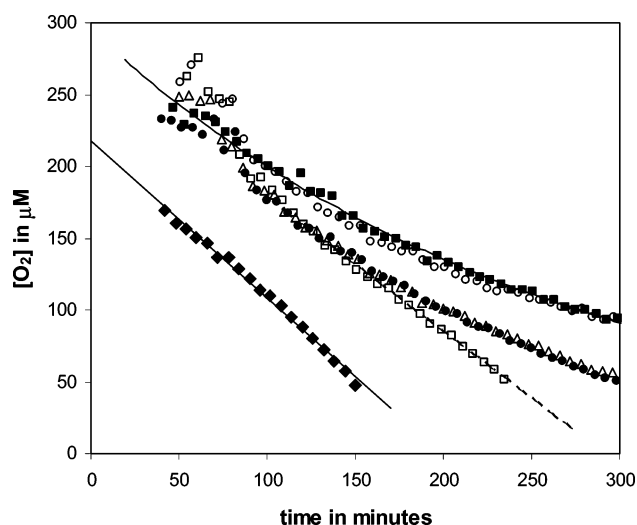


**Figure 6.** Oxygen consumption by  $0.5 \times 10^6$  Jurkat cells/mL exposed to  $20 \mu\text{M}$  total dactinomycin + doxorubicin. Filled diamonds and line, cells alone (with linear fit); open squares and dashed line, cells plus  $20 \mu\text{M}$  doxorubicin (with linear fit to points after 120 min); triangles, cells plus  $15 \mu\text{M}$  doxorubicin plus  $5 \mu\text{M}$  dactinomycin; open circles,  $10 \mu\text{M}$  doxorubicin plus  $10 \mu\text{M}$  dactinomycin; filled circles, cells plus  $5 \mu\text{M}$  doxorubicin plus  $15 \mu\text{M}$  dactinomycin; filled squares and curved line, cells plus  $20 \mu\text{M}$  dactinomycin (with exponential fit).

triangles, respectively) were fitted to exponentials (dashed and dotted lines, respectively) to show the curvature, which was larger for the higher concentration. The results for exposure to  $10 \mu\text{M}$  dactinomycin plus  $10 \mu\text{M}$  doxorubicin are shown by stars. The plot shows curvature, like the two preceding, and closely follows the corresponding plot for  $10 \mu\text{M}$  dactinomycin alone. For the purpose of comparison, we fit the points for  $t > 200$  min to straight lines. The slope for  $10 \mu\text{M}$  doxorubicin was then  $-0.978 \mu\text{M O}_2 \text{ min}^{-1}$ , for  $10 \mu\text{M}$  dactinomycin  $-0.525 \mu\text{M O}_2 \text{ min}^{-1}$ , for  $20 \mu\text{M}$  dactinomycin  $-0.634$ , and for  $10 \mu\text{M}$  dactinomycin +  $10 \mu\text{M}$  doxorubicin  $-0.765 \mu\text{M O}_2 \text{ min}^{-1}$  ( $r^2 = 0.997, 0.997, 0.998, \text{ and } 0.995$ , respectively). Because the slope for untreated cells was  $-0.973 \mu\text{M O}_2 \text{ min}^{-1}$ ,  $10 \mu\text{M}$  dactinomycin,  $20 \mu\text{M}$  dactinomycin, and  $10 \mu\text{M}$  dactinomycin +  $10 \mu\text{M}$  doxorubicin lowered respiration by 46%, 35%, and 19%, respectively.

We conducted another series of studies using  $20 \mu\text{M}$  total drug but with different concentrations of dactinomycin and doxorubicin. Again,  $0.5 \times 10^6$  Jurkat cells were used, with the following conditions: (1) cells alone, (2) cells plus  $20 \mu\text{M}$  doxorubicin, (3) cells plus  $15 \mu\text{M}$  doxorubicin plus  $5 \mu\text{M}$  dactinomycin, (4) cells plus  $10 \mu\text{M}$  doxorubicin plus  $10 \mu\text{M}$  dactinomycin, (5) cells plus  $5 \mu\text{M}$  doxorubicin plus  $15 \mu\text{M}$  dactinomycin, and (6) cells plus  $20 \mu\text{M}$  dactinomycin. The results are shown in Figure 6. For untreated cells (solid diamonds), the slope of the best-fit line ( $r^2 = 0.994$ ) was  $-1.098 \mu\text{M O}_2 \text{ min}^{-1}$ . The results for  $20 \mu\text{M}$  doxorubicin (open squares) fit well with two lines meeting at 120 min; the line for  $t > 120$  min (dashed line) had a slope of  $-0.929 \mu\text{M O}_2 \text{ min}^{-1}$ , representing a 15% decrease in respiration.

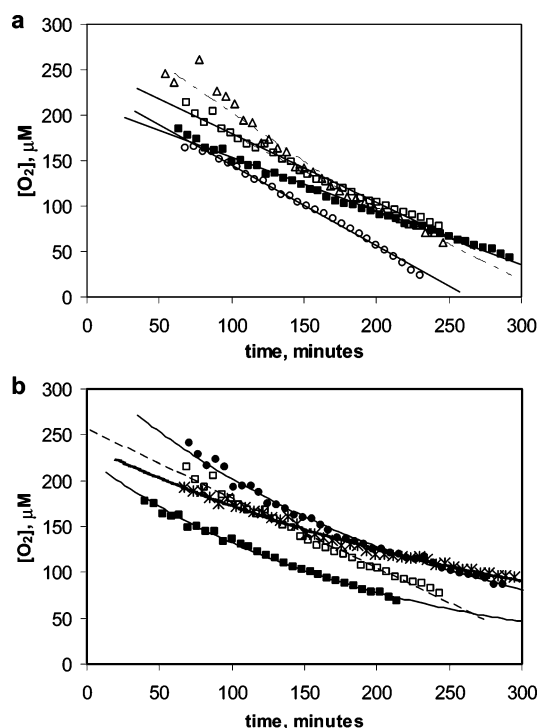


**Figure 7.**  $[\text{O}_2]$  as a function of  $t$  for  $0.5 \times 10^6$  HL-60 cells in the presence of dactinomycin and/or doxorubicin. (a) Circles with best-fit straight line, untreated cells; open squares with best-fit straight line,  $10 \mu\text{M}$  doxorubicin, filled squares with best-fit straight line,  $10 \mu\text{M}$  dactinomycin, triangles with broken line,  $20 \mu\text{M}$  doxorubicin. The broken line is obtained by fitting  $[\text{O}_2]$  vs  $t$  to two lines, one for  $t < 148$  min and one for  $t > 148$  min. (b) Open squares and dashed line,  $10 \mu\text{M}$  doxorubicin with linear fit; filled squares and solid line,  $10 \mu\text{M}$  dactinomycin with exponential fit; filled circles and solid line,  $10 \mu\text{M}$  dactinomycin +  $10 \mu\text{M}$  doxorubicin with exponential fit; asterisks and heavy line,  $20 \mu\text{M}$  dactinomycin with exponential fit.

For conditions 3–6, the plots of  $[\text{O}_2]$  versus  $t$  showed gradual curvature (an exponential fit to the results for  $20 \mu\text{M}$  dactinomycin is shown in Figure 6). To compare respiration rates, we fitted the points for  $t > 175$  min to lines. For conditions 3–6, the slopes were  $-0.491 \mu\text{M O}_2 \text{ min}^{-1}$  ( $r^2 = 0.996$ ),  $-0.377 \mu\text{M O}_2 \text{ min}^{-1}$  ( $r^2 = 0.975$ ),  $-0.537 \mu\text{M O}_2 \text{ min}^{-1}$  ( $r^2 = 0.996$ ), and  $-0.417 \mu\text{M O}_2 \text{ min}^{-1}$  ( $r^2 = 0.986$ ), respectively. All represented a much greater decrease in respiration relative to no drug (55%, 66%, 51%, and 62%, respectively) than that obtained from doxorubicin alone. The decrease in respiration was about the same in all four cases. Thus, increasing the fraction of dactinomycin in the mixture, with a total drug concentration of  $20 \mu\text{M}$ , had little effect. However, in the presence of dactinomycin the oxygen-consumption plot seems to have the gradual curve characteristic of dactinomycin and not the broken-line pattern characteristic of doxorubicin.

Similar results are obtained for HL-60 cells treated with dactinomycin and/or doxorubicin, as shown in Figure 7. In Figure 7a, open circles are  $[\text{O}_2]$  versus  $t$  for untreated cells. The best-fit line shown ( $r^2 = 0.995$ ) has a slope of  $-0.881$

$\mu\text{M O}_2 \text{ min}^{-1}$ . Open squares are for cells treated with  $10 \mu\text{M}$  doxorubicin. The best-fit line shown ( $r^2 = 0.985$ ) has a slope of  $-0.755 \mu\text{M O}_2 \text{ min}^{-1}$ , showing that this concentration of doxorubicin has little effect, reducing the respiration rate by less than 15%. The effect of  $10 \mu\text{M}$  dactinomycin (filled squares) is much more pronounced: the best-fit line ( $r^2 = 0.993$ ) has a slope of  $-0.587 \mu\text{M O}_2 \text{ min}^{-1}$ , corresponding to a reduction in respiration by  $1/3$ . The triangles are for cells exposed to  $20 \mu\text{M}$  doxorubicin. As expected, the  $[\text{O}_2]$ -versus- $t$  curve is well fit by two lines (see Figure 7a). The line for  $t < 150 \text{ min}$  has a slope of  $(-1.08 \pm 0.13) \mu\text{M O}_2 \text{ min}^{-1}$ , and the line for  $t > 150 \text{ min}$  has a slope of  $(-0.80 \pm 0.02) \mu\text{M O}_2 \text{ min}^{-1}$ .

Figure 7b shows the results for  $10 \mu\text{M}$  doxorubicin (open squares) and  $10 \mu\text{M}$  dactinomycin (filled squares) again, but an exponential fit is shown for the latter. The exponential fit,  $[\text{O}_2] = 223e^{-0.0052t}$ , has  $r^2 = 0.9947$ , noticeably better than  $r^2 = 0.9926$  found for the linear fit of Figure 7a, confirming the continuous decrease in  $k$  observed with dactinomycin. The asterisks are for cells treated with  $20 \mu\text{M}$  dactinomycin, with the best-fit exponential (shown as heavy line),  $[\text{O}_2] = 238 e^{-0.0032t}$  ( $r^2 = 0.989$ ). The best linear fit to these data has  $r^2 = 0.972$ , showing that the curvature is much more important at the higher dactinomycin concentration. Finally, the solid circles are for cells treated with  $10 \mu\text{M}$  dactinomycin +  $10 \mu\text{M}$  doxorubicin, with the exponential fit,  $[\text{O}_2] = 318e^{-0.0045t}$  ( $r^2 = 0.9925$ ). The best linear fit to these data has  $r^2 = 0.9609$ , indicating that the oxygen curve for the mixed drugs has the characteristic shape obtained with dactinomycin. It may be noted that the exponential parameter (0.0045) is not very different from the exponential parameters for  $10 \mu\text{M}$  and  $20 \mu\text{M}$  dactinomycin (0.0052 and 0.0032, respectively).

**Calculating Respiration Rates.** We have defined the respiration rate,  $k$ , as the negative of the slope of the curve of  $[\text{O}_2]$  versus  $t$ . Dividing by the number of cells gives a rate in  $\mu\text{M O}_2 \text{ min}^{-1}$  per  $10^6$  cells. It is meaningful to multiply this by the reaction volume (1 mL in the present experiments) and obtain  $k$  in  $\text{nmol O}_2 \text{ min}^{-1}$  per  $10^6$  cells. In the presence of dactinomycin, the respiration rate decreased gradually with  $t$ , as evidenced by the positive curvature in the plots of  $[\text{O}_2]$  versus  $t$ , such as those seen in Figure 2b, 3b, and 6. These plots could be well fit by the three-parameter quadratic form,  $[\text{O}_2] = \alpha + \beta t + \gamma t^2$ ; going to the four-parameter cubic form did not improve the fit. Thus, to obtain the derivative  $d[\text{O}_2]/dt$  for cells exposed to dactinomycin, we fit a plot of  $[\text{O}_2]$  versus  $t$  to  $\alpha + \beta t + \gamma t^2$  and calculate  $k$  as  $-(\beta + 2\gamma t)$  divided by the number of cells and multiplied by the reaction volume. To this approximation,  $k$  is a linear function of  $t$ . (Because  $k$  should be constant in the absence of drug, we fit the  $[\text{O}_2]$ -versus- $t$  plot for zero drug concentration to a line and obtain  $k$  from the slope; it is of course  $t$ -independent.)

Theoretically,  $k$  should be the same for all samples at  $t = 0$ , before the effect of drug is felt. In reality, errors in sampling will lead to different values of  $k$  at  $t = 0$ . We correct for these errors by multiplying each calculated  $k$  by a constant to bring it into coincidence with  $k$  for untreated

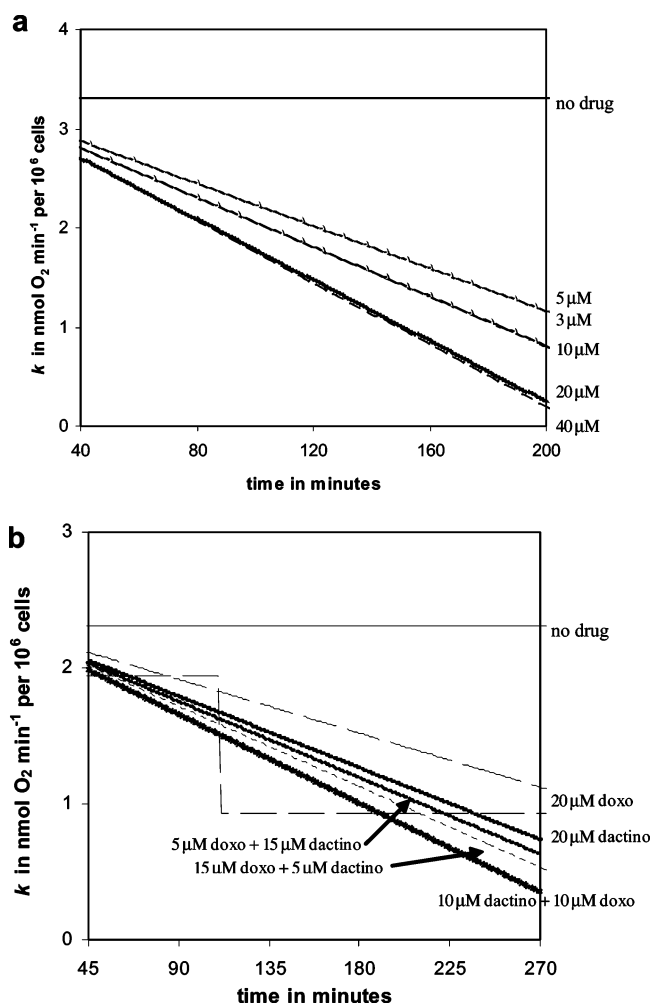


**Figure 8.** Respiration rate constants,  $k$ , calculated from plots of  $[\text{O}_2]$  vs  $t$  by fitting the data to the quadratic form  $\alpha + \beta + \gamma t^2$ , differentiating with respect to  $t$ , dividing by the number of cells, and multiplying by the reaction volume. All curves have been normalized to give the same  $k$  at  $t = 0$ , the value obtained in the absence of the drug. (a) Values of  $k$  obtained for cells exposed to various [dactinomycin] (Figure 2a and b). From top to bottom, the plots correspond to [dactinomycin] = 0, 5, 3, 10, 40, and  $20 \mu\text{M}$ ; the curves for 5 and  $3 \mu\text{M}$ , and those for 20 and  $40 \mu\text{M}$ , are virtually indistinguishable. (b) Values of  $k$  obtained for cells exposed to  $20 \mu\text{M}$  drug (Figure 6). From top to bottom: no drug,  $20 \mu\text{M}$  doxorubicin,  $20 \mu\text{M}$  dactinomycin,  $15 \mu\text{M}$  dactinomycin +  $5 \mu\text{M}$  doxorubicin,  $5 \mu\text{M}$  dactinomycin +  $15 \mu\text{M}$  doxorubicin, and  $10 \mu\text{M}$  dactinomycin +  $10 \mu\text{M}$  doxorubicin. The step function is the  $k$  value obtained by fitting the  $[\text{O}_2]$  results for  $20 \mu\text{M}$  doxorubicin to two straight lines.

cells at  $t = 0$ . This procedure yields the plots in Figure 8. Note that the use of quadratic fitting functions makes the plots only a rough approximation of  $k$ .

Figure 8a shows the  $k$  values obtained from the oxygen plots of Figure 2a and b. From top to bottom, the plots correspond to [dactinomycin] = 0, 5, 3, 10, 40, and  $20 \mu\text{M}$ ; the curves for 5 and  $3 \mu\text{M}$ , and those for 20 and  $40 \mu\text{M}$  are virtually indistinguishable. As expected, the respiration rate constant,  $k$ , was lowered more quickly for higher [dactino-

mycin]; discrepancies existed because of the approximations made in obtaining the  $k$ -versus- $t$  curves. The near-coincidence of the 20 and 40  $\mu\text{M}$  curves suggests that saturation occurs. The  $t$  at which  $k$  becomes zero, roughly 220 min for 20 or 40  $\mu\text{M}$ , is the  $t$  at which respiration for these cells is completely halted by continuous exposure to the drug.

Figure 8b shows the  $k$  values obtained from the oxygen plots of Figure 6, which correspond to continuous exposure to dactinomycin–doxorubicin mixtures with 20  $\mu\text{M}$  total drug. The horizontal line (constant  $k$ ) is for cells not treated with drug. The next lines (for more rapidly decreasing  $k$ ) are for 20  $\mu\text{M}$  doxorubicin, 20  $\mu\text{M}$  dactinomycin, 15  $\mu\text{M}$  dactinomycin + 5  $\mu\text{M}$  doxorubicin, 5  $\mu\text{M}$  dactinomycin + 15  $\mu\text{M}$  doxorubicin, and 10  $\mu\text{M}$  dactinomycin + 10  $\mu\text{M}$  doxorubicin. It is clear that 20  $\mu\text{M}$  doxorubicin inhibits respiration much less than 20  $\mu\text{M}$  dactinomycin or any of the drug mixtures. However, 20  $\mu\text{M}$  dactinomycin is no more effective at inhibiting respiration than 10:10 or 5:15 drug mixtures. Thus, the effects of the drugs are not additive; it seems that a small admixture of dactinomycin increases the ability of doxorubicin to inhibit respiration. Indeed, the fact that the  $k$  values for the drug mixtures are below  $k$  for 20  $\mu\text{M}$  dactinomycin suggests that the drugs act synergistically, the presence of doxorubicin augmenting the respiration-inhibiting power of dactinomycin.

As mentioned previously, the effect of doxorubicin on mitochondrial respiration seems to be abrupt: the respiration rate remains unchanged for about 2 h, after which it decreases markedly and remains constant thereafter. We have fitted the  $[\text{O}_2]$ -versus- $t$  curve for 20  $\mu\text{M}$  doxorubicin to two straight lines, taking the intersection of the lines as one of the variable parameters. The resulting  $k$  value, which is equal to 1.883 for  $t < 121$  min and 0.920 for  $t > 121$  min, is shown in Figure 8b as a broken line.

## Discussion

We report here measured cellular mitochondrial oxygen consumption (Figures 2 and 3) and ATP content (Figure 4) during continuous exposure to dactinomycin. We show that the drug inhibits respiration and lowers ATP content in Jurkat and HL-60 cells. The effect of dactinomycin on respiration is greater than that of doxorubicin at the same concentration. For both drugs, the inhibition of respiration is greater for higher drug concentrations. As a result, profound cellular ATP depletion occurs within 3–4 h of drug exposure. The presence of cyanide in these experiments inhibits respiration (Figure 2d) and ATP content (see Results), establishing that both processes occurred primarily in the mitochondrial respiratory chain. Although we view the decrease in ATP levels in the presence of dactinomycin as a consequence of the inhibition of respiration by the drug, it is possible that there is a direct effect of the drug on the enzymes catalyzing ATP formation or hydrolysis, or other components of mitochondrial function.

We utilized the pancaspase family inhibitor zVAD-fmk<sup>8</sup> to investigate whether these apoptosis-associated proteases mediated the inhibitory effects of dactinomycin on respira-

tion. Although zVAD-fmk in fact blocked the dactinomycin-induced decrease in oxygen consumption (Figure 2c), it also produced a decrease in ATP level within 1 h of addition (Figure 4a). This decrease was shown to be an effect of DMSO, introduced along with the zVAD-fmk; cellular leakage of ATP may have been involved. The level of ATP subsequently recovered, showing that zVAD-fmk did prevent dactinomycin from decreasing cellular ATP. It is clear from these observations (Figures 2–4) that the dactinomycin-induced inhibition of respiration and ATP formation require caspase activities. Thus, the results shown in Figures 2–4 clearly describe the onset and severity of mitochondrial dysfunction during dactinomycin-induced apoptosis. The data also suggest that oxidative phosphorylation remains intact during the formation of apoptosomes and prior to caspase activation.

The precise mechanism of caspase-mediated impairment of cellular respiration (inhibition of mitochondrial oxygen consumption and accompanying ATP synthesis) remains unknown. In addition to directly inhibiting oxidative phosphorylation, these proteases may impair other critical processes in ATP synthesis and hydrolysis. However, despite the fact that doxorubicin is known to interfere with components of the mitochondrial respiratory chain, this direct effect of the drug appears to be less important than the caspase-mediated insults.

For the same concentration, dactinomycin is a more potent inhibitor of respiration than doxorubicin. Furthermore, we show that cells treated with dactinomycin exhibit gradually decreasing respiration (Figure 2b), unlike cells treated with doxorubicin, for which there is an abrupt decrease.<sup>10</sup> The different shapes of the plots of  $[\text{O}_2]$  versus  $t$  produced by the two drugs (Figures 5 and 6) suggest that each drug executes cell death (apoptosis or necrosis) and interferes with the respiratory chain in a different way. Dactinomycin may induce cell death (apoptosis or necrosis) in a part of the population after a short incubation time, and in more of the population with longer times, whereas doxorubicin has little or no effect until  $\sim 100$  min, at which time a substantial fraction of the cells die.

Experiments in which Jurkat cells were incubated with mixtures of the two drugs, with the same total concentration, were also of interest. When the two drugs were used together, their effects were not at all additive; each drug seemed to enhance the action of the other. The significance of this finding remains to be explored further. The oxygen-consumption curves in the presence of both drugs resemble those for dactinomycin alone. This is not surprising: dactinomycin exerts some effects at early times. Later, when the abrupt drop in  $k$  produced by doxorubicin<sup>10</sup> should occur,  $k$  is so small that it would be difficult to detect the change in slope.

Observations relevant to the role of mitochondrial  $\Delta\psi$  were presented in a series of reports by Green and co-workers,<sup>6,7,9,15–16</sup> who examined the apoptotic response of HL-60 and other cells following short exposures to dactinomycin, etoposide, or staurosporine. Apoptosis was initiated

without noticeable changes in  $\Delta\psi$ , which occurred only later in the cell-death process.<sup>15</sup> Studies of single cells treated with etoposide or dactinomycin showed that, if caspases were not activated, the mitochondria maintained generation of ATP even after the release of cytochrome *c*.<sup>16</sup> In contrast, caspase activation disrupted complexes I and II of the mitochondrial electron transport chain, resulting in diminished  $\Delta\psi$  and generation of reactive oxygen species.<sup>6</sup> The results in Figures 2–4 agree with these reports and show that caspase activation impairs oxidative phosphorylation. The observed decrease in cellular ATP (Figure 4) emphasizes the importance of the mitochondrial cell-death pathway during apoptosis;<sup>5</sup> that is, the energy-converting processes shut down in cells exposed to high concentrations of toxins.

- 
- (15) Finucane, D. M.; Waterhouse, N. J.; Amarante-Mendes, G. P.; Cotter T. G.; Green, D. R. Collapse of inner mitochondrial transmembrane potential is not required for apoptosis of HL60 cells. *Exp. Cell Res.* **1999**, *251*, 166–174.
- (16) Waterhouse, N. J.; Goldstein, J. C.; von Ahsen, O.; Schuller, M.; Newmeyer, D. D.; Green, D. R. Cytochrome *c* maintains mitochondrial transmembrane potential and ATP generation after outer mitochondrial membrane permeabilization during the apoptotic process. *J. Cell Biol.* **1999**, *153*, 319–328.

In isolated mouse liver mitochondria, oxygen uptake in response to substrates for complex I or II of the respiratory chain was inhibited in the presence of exogenous cytochrome *c*, tBid, and caspase-3. In contrast, oxygen uptake in response to substrates for complex IV remained intact. Somewhat similar results were observed in Jurkat cells treated with etoposide or staurosporine.<sup>6</sup> Moreover, in permeabilized HeLa cells, loss of  $\Delta\psi$  and generation of reactive oxygen species were observed in the presence of caspase-3 and substrates for complex I or II, but not for those of complex IV.<sup>6</sup> In HeLa cells treated with 1.0  $\mu$ M dactinomycin, loss of  $\Delta\psi$  was observed at about 2 h and recovery about 30–60 min later. In Jurkat cells, incubation with 0.5 mM dactinomycin produced more than 60% apoptosis by 8 h.

In summary, the results presented here show that cells exposed to dactinomycin exhibit dose-dependent impairment of oxidative phosphorylation, which result from caspase activation.

**Acknowledgment.** This work was supported by a fund from the Paige's Butterfly Run. Thanks are due to Ms. Bonnie Toms for her help with the cell cultures.

MP0600485